

**Effects of One-Way and Two-Way Directional Heavy Vehicle Simulator Loading on Rutting in Hot Mix Asphalt Pavements**

Marc Novak  
University of Florida  
Graduate Student  
Department of Civil and Coastal Engineering  
P.O. Box 116580  
Gainesville, FL 32611-6580  
Telephone: (352) 392-9537  
Fax: (352) 392-3394  
E-mail: men@ufl.edu

Dr. Bjorn Birgisson  
(Corresponding Author)  
University of Florida  
Assistant Professor  
Department of Civil and Coastal Engineering  
P.O. Box 116580  
Gainesville, FL 32611-6580  
Telephone: (352) 392-9537  
Fax: (352) 392-3394  
E-mail: bbirg@ce.ufl.edu

Dr. Reynaldo Roque  
Professor  
Department of Civil Engineering, University of Florida  
345 Weil Hall, P. O. Box 116580  
Gainesville, FL 32611-6580  
Tel: (352) 392-9537 ext. 1458  
Fax: (352) 392-3394  
Email: rroqu@ce.ufl.edu

Dr. Bouzid Choubane  
Florida Dept. of Transportation  
Materials Research Park  
5007 N.E. 39th Avenue  
Gainesville, FL 32609  
Phone: (352) 955-6302  
Fax: (352) 955-6345  
E-mail: bouzid.choubane@dot.state.fl.us

Word Count: 7160 words [abstract (170) + text (3740) plus 4 tables and 9 figures]

Revised Nov 14, 2004 for January 2004 TRB Annual Meeting and Subsequent Publication

**Abstract.** Instability rutting generally occurs within the top five centimeters (two inches) of the asphalt layer when the structural properties of the asphalt concrete are inadequate to resist the stresses imposed upon it. It is generally believed that near-surface transverse shear stresses perpetuate instability rutting. Field observations of Heavy Vehicle Simulator (HVS) testing noted greater rutting in one-way directional loading compared to two-way directional loading, even at lower temperatures and with longer rest periods between load applications. An analysis of stress states in the asphalt pavement layer using the three-dimensional finite element commercial code ADINA showed that longitudinal stress path patterns varied between the different directional loadings. A hypothesis was developed that the differences in longitudinal plane stress path patterns between one-way and two-way directional loading attributed to the different levels of rutting. A visco-elastic model with load applications simulating the different directional loadings was constructed and used to test this hypothesis. The visco-elastic model results indicated qualitatively that even with greater relaxation times, one-way directional loading produces greater strains.

Keywords: Instability Rutting, Heavy Vehicle Simulator, Finite Element Analysis, Stress Path Patterns

## INTRODUCTION

Rutting is a major distress mode in hot mix asphalt (HMA) pavements. Rutting is the mechanism that produces depressions within the wheel path, reducing serviceability and increasing the potential of hydroplaning. Ruts may be caused by volumetric compression and/or shear deformation. Traditionally, rut prediction was based on the strength and stiffness of the subgrade alone (1). However, rutting has been observed to occur in the HMA layer only, typically the top 50 mm (2 in) resulting from lateral movement of the asphalt. Rutting that is confined to the HMA layer is known as instability rutting (2,3) and generally shows itself during the first hot summer. The driving mechanism behind instability rutting is thought to be high tire inflation pressures and high near surface shear stresses at low confinements amplified by today's radial tires (4,5). Instability rutting is therefore not a pavement structural issue but a mixture issue.

The Florida Department of Transportation (FDOT) recently conducted an evaluation on the most efficient method of Heavy Vehicle Simulator (HVS) loading at the Accelerated Pavement Testing (APT) facility in Gainesville, Florida. This study investigated the HVS tire wander and one-way versus two-way directional tire loading. The results clearly showed that one-way directional loading resulted in faster rut progression and in greater rut depths. The uni-directional loading caused the rut to develop at a rate of approximately 65 percent greater than that of the bi-directional loading. Also, the one-way loading sections had slightly lower average temperatures than the two-way loading sections (6,7,8) suggesting that if the temperatures between the sections had been the same, the differences would have been even more striking. Differences in rutting from one-way or two-way directional loading have not been observed at low temperatures (9). It is important to note that the rutting that occurred was indeed instability rutting. Trench cuts conducted after testing showed that there had been no deformation of the base layer; rutting was confined to the asphalt layer only i.e., true instability rutting.

The directional testing results raised two questions. First, it is well known that asphalt concrete exhibits visco-elastic properties (11). In two-way directional loading, the relaxation time is about half that of the one-way directional loading. A greater relaxation time should provide time to recover more delayed elastic strains, but actually the one-way directional loading with greater relaxation times between passes produces the greater rutting. Second, if instability rutting is thought to be due to shoving near the surface caused primarily by transverse shear stresses near the edges of the wheel-path (1,3,10), then there should be little difference in the rut depths between one and two-way directional loading. Stresses in the longitudinal plane must also have an effect on the degree of rutting. The stress paths occurring in the longitudinal plane of the asphalt layer under one-way directional loading may provide a one-way kneading action of the hot mix asphalt resulting in higher degrees of rutting, as compared to two-way directional loading, which "kneads" the hot mix asphalt in a back and forth action.

## OBJECTIVES

HVS testing demonstrated that one-way directional loading produces greater rut depths than two-way directional loading. The objectives of this paper are as follows:

- To employ three-dimensional finite element analysis to obtain stress paths induced in the asphalt layer of a typical pavement system from a Super-single radial tire.
- To evaluate and illustrate the differences in stress path patterns in the asphalt layer between one-way and two-way directional loading.
- To evaluate the differences the stress path patterns of one-way and two-way directional loading have on the deformation of a simple visco-elastic model representing asphalt concrete.

## SCOPE

This paper provides an analysis of typical three-dimensional stress states associated with a typical radial truck tire. The paper identifies critical transverse and longitudinal stress states. It is hypothesized that the differences in rut depths between one-way and two-way directional loading must be due to differences in stress paths in the asphalt layer. Furthermore, the differences in the stress paths between one-way and two-way directional loading must explain the greater rutting in a visco-elastic material with greater relaxation times. This paper provides an explanation of the differences between one-way and two-way directional rutting. Knowledge obtained will offer insights into the mechanisms of instability rutting.

### One-way versus Two-way Directional Loading Analysis

Instability rutting is initially primarily volumetric, but then is predominantly propagated by shear movement (12). The area believed most critical to the propagation of instability rutting is the near surface on the outside edge of the tire at depths of no more than 50 mm (2 in) where shear stresses are the highest (3,4,5). This section identifies the similarities and differences in stress path and stress cycles, both qualitatively and quantitatively through three-dimensional finite element analysis, for one-way and two-way HVS directional loading in the critical locations of instability rutting.

### Three-Dimensional Finite Element Analysis

A three-dimensional finite element analysis using the commercial code ADINA (13) was used for the analysis of the asphalt pavement stresses due to HVS loading by modeling a super-single radial tire. The HVS used a super-single radial tire with an average contact stress of 792 kPa (115 psi) and a footprint of 305 mm (12 in) wide by 203 mm long (8 in) (8). Since the exact tire contact stresses were not known for the radial tire used in the HVS, typical available tire contact stress data on a 230 mm (9 in) wide by 153 mm (6in) long super-single radial tire rated at 792 kPa (115 psi) was available and was used in the analysis (4,5). Tire contact stresses were based on a tire contact measurement system developed by M.G. Pottinger (14), which was especially developed for tire research, and consists of 1200 distinct measurement points, which register contact stresses in the x, y and z directions. This resulted in over 3,600 distinct stress measurements for the nine-inch wide super-single tire radial tire with five ribs and a gross contact area of 300 cm<sup>2</sup> (47 in<sup>2</sup>) with an inflation pressure of 792 kPa (115 psi). The measurements provided a high definition of actual tire contact stresses.

The challenge in modeling stresses in the asphalt layer due to a radial tire is that the radial tire contact area is rather small and highly non-uniform. The pavement structure at the HVS testing site consisted of a 100 mm (4 in) thick thin layer of unmodified SP-12.5 mm asphalt concrete, overlying a 270 mm (10.5 in) limerock base and a 300 mm (12 in) thick limerock stabilized sub-base, which rests on a semi-infinite sandy subgrade. Hence, the combination of a small, highly non-uniformly loaded contact area and relatively thin surface layers, connecting to a semi-infinite half plane requires a large number of elements.

An initial assessment of the grid size requirements based on using a uniform stress distribution demonstrated that the three-dimensional model should be at least 1800 mm (70 in) deep and extend laterally at least 1500 mm (60 in) in each direction from the center of the tire contact load to adequately represent the semi-infinite half space conditions associated with pavement problems. To overcome the limitations associated with building a traditional mesh, contact surfaces were introduced, where a fine graded mesh representing the loaded surface was attached (“glued”) onto a coarse-graded mesh. The fine-graded mesh was used around the loaded area for this was the region of interest. Coarse meshes were used at distances further away from the loaded area where the change in stress was more gradual and the stresses in these regions were not of much concern for instability rutting. Contact surfaces were used for the transition from the asphalt layer to the base, from the base to the foundation, and from the fine mesh near the tire contact area to the peripheral areas.

The measured tire contact measurements reported tire contact stresses as uniform stresses acting over areas of 0.2 cm<sup>2</sup> (0.03 in<sup>2</sup>) in size. Three different stresses were provided, namely vertical normal stresses, transverse shear stresses, and longitudinal shear stresses. Ideally, each uniform stress should be applied to a single element. Unfortunately, the number of elements needed would have exceeded the memory of the Silicon Graphics multi-processor supercomputer available for the analysis. Thus, the use of fewer elements was required under the contact area, which subsequently required the determination of the equivalent nodal forces to be applied to each node. The appropriate nodal forces for each element were determined by converting each uniform stress into an equivalent concentrated force through the use of shape functions (15).

The final three-dimensional mesh consisted of 204,185 nodes—with three degrees of freedom per node, resulting in a total of 612,555 degrees of freedom. The elements under the radial contact area had uniform dimensions of 7.62 mm by 10.16 mm (0.3 by 0.4 inches). Figure 1 illustrates the final three-dimensional mesh, with Figure 2 showing a plan view of the contact area of the three-dimensional mesh.

Although flexible pavement materials are generally nonlinear in nature, a firm understanding of the linear elastic stress states should precede more complicated nonlinear analysis. In the following, all pavement layers are assumed to be linear elastic, and dynamic effects are ignored in favor of promoting a basic understanding of static stress states before complicating the analysis with dynamic effects. Table 1 lists the elastic moduli, Poisson’s ratio and layer thickness of the pavement layers used in the analysis. The modulus for the asphalt concrete was

determined from IDT resilient modulus tests at 25°C on the same unmodified asphalt concrete used in the testing—close to the average ambient testing temperature in the directional loading analysis (6,7). The base and subgrade values were based on LBR values conducted by the FDOT and converted to modulus values using the 1986 AASHTO formula (16). The Poisson's ratio was selected to ensure minimal volumetric changes, to simulate a moving tire load during the shear-driven phase of instability rutting.

As previously mentioned, the area in the asphalt layer most critical to instability rutting is the upper two inches near the edge of the tire as depicted in Figure 3. Figures 4 and 5 display the transverse YZ-plane and longitudinal XZ-plane shear stress magnitudes in the longitudinal wheel travel directional from the finite element analysis along the edge of the tire at depths of 10, 25, 40 mm (0.5, 1, and 1.5 in). Idealized depictions of the shear deformation for an element in the asphalt layer under the shear magnitudes reported are presented with the lettering in Figures 4 and 5. The maximum shear stress in the longitudinal XZ-plane, seen in Figure 5, produces shear stresses about one-half of the maximum shear stress in the transverse YZ-plane, shown in Figure 4. It is also interesting to note that the maximum shear stresses occur at depths of 40 mm and shear stresses do not vary much in the top 40 mm.

Transverse YZ-plane shear stresses near the edge of the wheel-path will undergo shearing only in one direction as the wheel approaches and passes -- increasing in magnitude as the wheel approaches and decreasing in magnitude as the wheel passes. This shear pattern is illustrated in Table 3. The elements labeled A, B, and C in Figure 4 also depict the shearing pattern experienced by an element in the asphalt layer under these transverse shear stresses. This pattern of A-B-C transverse shear stress reversal is repeated for an element in the asphalt layer on the edge of the wheel-path no matter whether under one-way or two-way directional loading. Two passes in one-way directional loading would result in a shear stress pattern of A-B-C – A-B-C in the asphalt layer, while two passes in two-way directional loading would result in a stress pattern of A-B-C – C-B-A in the asphalt layer. The magnitude of B would not vary between passes or upon the one-way or two-way directional loading. Thus, there is no difference between the shear stress pattern in the transverse YZ-plane between one-way and two-way directional loading.

The differences between one-way and two-way directional loading are however manifested in the shear stress patterns in the longitudinal XZ-plane. Elements in the XZ-plane undergo a stress pattern depicted in Figure 6. The sheared elements labeled A, B, C, D, and E in Figures 5 and 6 also depict this pattern of shearing. For a cycle of two passes in two-way loading, an element on the edge of the wheel path in the asphalt layer will experience a shear stress path pattern of: A-B-C-D-E – E-D-C-B-A. For a cycle of two passes in one-way loading, an element in the asphalt layer will experience a pattern a shear stress pattern of: A-B-C-D-E – A-B-C-D-E. The magnitudes of the shear are equal but in opposite directions for positions B and D.

In summary, in two-way loading, the shear stress reverses not only from positive to negative, but the shear stress path pattern reverses from positive to negative to negative to positive. It is this shear stress path pattern reversal that distinguishes two-way loading from one-way loading in the HVS.

## Investigation

To determine whether the lack of the shear stress path pattern reversal, as seen in one-way loading, has an effect on permanent deformation, a simple analytical model was designed. Asphalt concrete is a complex material that seldom exhibits solely elastic deformation. Deformations in asphalt concrete typically contain viscous, visco-elastic and plastic deformations in addition to the elastic deformations. A simple model that can employ visco-elastic deformations, including permanent creep deformations, is the Burgers Model, also known as the four-element model (11). The Burgers Model has the advantages of capturing instantaneous and delayed elastic deformation responses upon loading as well as instantaneous, delayed, and permanent deformation responses upon unloading. The Burgers Model is simply a Maxwell and a Kelvin Model connected in series, as shown in Figure 8 (17).

The constitutive equation for the Burgers Model is described below. Four properties are required, two elastic constants representing the elastic modulus ( $R_1$  and  $R_2$ ) and two viscous constants ( $\eta_1$  and  $\eta_2$ ). The total strain at time  $t$  will be the sum of the strains from the spring and dashpot in the Maxwell Model and the strain in the Kelvin Model, as written below:

$$\varepsilon = \varepsilon_1 + \varepsilon_2 + \varepsilon_3 \quad (1)$$

where  $\varepsilon_1$  is the strain in the spring:

$$\varepsilon_1 = \frac{\sigma}{R_1} \quad (2)$$

and  $\varepsilon_2$  is the strain in the dashpot,  $\sigma$  is the applied stress:

$$\varepsilon_2^* = \frac{\sigma}{\eta_1} \quad (3)$$

and  $\varepsilon_3$  is the strain in the Kelvin part:

$$\dot{\varepsilon}_3 + \frac{R_1}{\eta_2} \varepsilon_3 = \frac{\sigma}{\eta_2} \quad (4)$$

These all can be combined to give the following constitutive equation:

$$\sigma + \left( \frac{\eta_1}{R_1} + \frac{\eta_1}{R_2} + \frac{\eta_2}{R_2} \right) \dot{\sigma} + \frac{\eta_1 \eta_2}{R_1 R_2} \ddot{\sigma} = \eta_1 \dot{\varepsilon} + \frac{\eta_1 \eta_2}{R_2} \ddot{\varepsilon} \quad (5)$$

The simplest way to obtain a solution is to use Laplace Transforms and their inverse. This has the advantage of simplicity and consistency. Applying the Laplace Transform to the above equations reduces them to algebraic expressions and transforms them into a function of the complex variable  $s$  instead of time ( $t$ ) indicated by a caret (^):

$$\hat{\sigma} + \left( \frac{\eta_1}{R_1} + \frac{\eta_1}{R_2} + \frac{\eta_2}{R_2} \right) s \hat{\sigma} + \frac{\eta_1 \eta_2}{R_1 R_2} s^2 \hat{\sigma} = \eta_1 s \hat{\varepsilon} + \frac{\eta_1 \eta_2}{R_2} s^2 \hat{\varepsilon} \quad (6)$$

The inverse Laplace transform will bring the above expression back into terms of  $t$ .

The Burgers Model was implemented into a MathCAD worksheet, representing asphalt concrete, to determine whether the reversal of the shear pattern (two-way loading) over a series of two cycles results in differences in total strain as compared to no reversal (one-way loading). The finite element stress path evaluation showed that an element in the upper inch of the asphalt layer does not experience shear stresses until the tire is 20.3 cm (8 inches) away. The maximum longitudinal shear stress achieved in the asphalt layer along the edges of the tire in the longitudinal plane is 103 kPa as shown in Figure 5. Assuming that the 203 mm (8 in) HVS radial tire used in the testing is traveling at the rated constant speed of 9.6 km/hr (6 mph), neglecting the deceleration and acceleration times for slow down and speed up when reversing direction, and the fact that the test track is thirty feet long, an element would experience a loading for about 0.22 seconds. The relaxation time between passes for the one-way loading would be 6.6 seconds and for the two-way loading would be 3.2 seconds.

A sinusoidal load, similar to the actual semi-triangular loading pattern found in the finite element analysis, with a peak stress of +103 and -103 kPa (+15 psi and -15 psi) was applied for 0.22 seconds. The next loading, representing the next pass, will either be +103 psi then -103 kPa for the one-way directional loading or -103 and +103 kPa (-15 psi and +15 psi) for the two-way directional loading, each with their respective relaxation times. Figures 9 and 10 (not to scale) display the loading patterns used in the analysis.

Properties for the Burgers Model were obtained from IDT creep tests (18) on a typical fine graded mix found in Florida similar to the one used in the HVS directional testing and are presented in Table 3.

The results from the different loading patterns with the Burger model are displayed in Table 4. The results show that the one-way directional loading produces more strain than the two-way directional loading in the one-dimensional Burger Model. The difference in strain for the one-way directional loading was two orders of magnitude greater than the two-way directional loading. Although the magnitude of the predicted deformations is higher than seen in the field, the differences match the observations that one-way directional loading produces more deformation than two-way directional loading.

## SUMMARY AND CONCLUSIONS

Near-surface rutting confined to the asphalt layer, also known as instability rutting, is a costly form of distress currently affecting roadways. This study investigated the nature of instability rutting observed in the HVS and the response of mixtures to instability rutting under one-way and two-way directional loading conditions.

HVS directional testing has demonstrated that there are differences in rut depth progression between one-way and two-way loading. Transverse shear stress patterns have no stress reversal and do not differ between one-way and two-way directional loading. Longitudinal shear stress patterns differ between one-way and two-way directional loading. There is a reversal of the shear stress pattern in two-way directional loading not seen in one-way directional loading. The shear stress pattern under one-way directional loading is positive to negative then positive to negative again, since the load is always approaching from the same direction. The shear stress pattern under two-way loading is positive to negative then negative to positive for each change in loading direction. This reversal occurs because the wheel in two-way loading is now approaching from the opposite direction.

The lack of shear stress pattern reversal (one-way loading) produces greater strain in a visco-elastic material model even with a greater relaxation time compared to one with shear pattern reversal and less relaxation time (two-way loading). The shear stress pattern reversal in the longitudinal planes found in two-way directional loading helps to “even out” strains resulting in less rutting. In one-way directional loading, the observed shear stress pattern reversal is not present allowing for the aggregate to continually “kneaded” and re-oriented in the same direction.

Instability rutting is a mode of distress that is manifested by lateral deformation in the transverse plane. Differences in the degrees of rutting between one-way and two-way HVS directional loading suggest that non-transverse stresses play a role in instability rutting propagation. Longitudinal shear stress path patterns from one-way HVS directional loading result in higher amounts of deformation in a viscoelastic material model than longitudinal shear stress patterns from two-way HVS directional loading. The field observations and the analysis imply that both transverse (primarily) and longitudinal (secondarily) plane shear stresses assist in the propagation of instability rutting. Three-dimensional analysis of the stress paths in the asphalt layer due to radial tires for different directional loadings offered an insight into the mechanisms behind instability rutting.

## REFERENCES

1. Huang, Y.H. *Pavement Analysis and Design*. Prentice-Hall, Inc., New York, 1993.
2. Dawley, C.B., Hogewiede, B.L., and K.O. Anderson. Mitigation of Instability Rutting of Asphalt Concrete Pavements in Lethbridge, Alberta, Canada. *Journal of the Association of Asphalt Paving Technologists*, Vol. 59, 1990, pp. 481-560.
3. Drakos, C., Roque, R., and B. Birgisson. Effect of Measures Tire Contact Stresses on Near-Surface Rutting. In *Transportation Research Record 1764*, TRB, National Research Council, Washington, D.C., 2001 pp. 59-69.
4. Novak, M., B. Birgisson, and R. Roque. Three-dimensional Finite Element Analysis of Measured Tire Contact Stresses and Their Effects on Instability Rutting in Asphalt Mixture Pavements. Accepted for Presentation and Publication at the 82nd Annual Transportation Research Board Meeting, Washington, D.C, 2003.
5. Novak, M., B. Birgisson, and R. Roque. Near Surface Stress States in Flexible Pavements using Measured Radial Tire Contact Stresses and ADINA. *Journal of Computers and Structures*, Vol. 81, 2003, pp. 859-870.
6. Tia, M., Byron, T., Sirin, O., Kim, H.J., and B. Choubane. Evaluation of Rutting Resistance of Superpave Mixtures with and without Modification by Means of Accelerated Pavement Testing. Accepted for Presentation and Publication at the 82nd Annual Transportation Research Board Meeting, Washington, D.C, 2003.
7. Tia, M., Roque, R., Sirin, O., H.J. Kim. *Evaluation of Superpave Mixtures With and Without Polymer Modification by Means of Accelerated Pavement Testing*. Final Report, University of Florida Project # 49104504801-12, 2002.
8. Byron, T., Choubane, B., and M. Tia. Assessing Appropriate Loading Configuration in Accelerated Pavement Testing. Accepted for Presentation and Publication at the 82nd Annual Transportation Research Board Meeting, Washington, D.C, 2003.
9. Huhtala, M. and J. Pihilajamaki. *HVS Nordic – The activity of the First period 1997-1999*. The Finnish National Road Administration Library, Helsinki, 2000.
10. Huber, G.A. *Methods to Achieve Rut-Resistance Durable Pavements*. Synthesis of Highway Practice 274, Transportation Research Board, National Research Council, Washington, DC, 1999.

11. Ullidtz, P. *Pavement Analysis*. Elsevier Science, New York, 1987.
12. Sousa, J.B., Crous, J., and C.L. Monismith. *Summary Report on Permanent Deformation in Asphalt Concrete*. Report SHRP-A/IR-91-104. Strategic Highway Research Program, National Research Council, Washington, D.C., 1991.
13. Bathe, K. ADINA system 7.5, User manual. Watertown, MA: ADINA R&D, Inc., 2001.
14. Pottinger MG. The three-dimensional contact stress field of solid and pneumatic tires. *Tire Science and Technology*, 1992; 20(1):3-32.
15. Novak, M., Birgisson, B. and R. Roque. Near surface stress states in flexible pavements using radial tire contact stresses and ADINA. *Journal of Computers and Structures*.
16. AASHTO. *Guide for Design of Pavement Structures*. American Association of American Highway and Transportation Officials, 1986.
17. Findley, W., Lai, J., and K. Onaran. *Creep and Relaxation of Nonlinear Viscoelastic Materials*. Dover Publications, Inc., New York, 1976.
18. Roque, R.L. and W.G. Buttlar. Development of a Measurement and Analysis System to Accurately Determine Asphalt Concrete Properties Using the Indirect Tensile Test. *Journal of the Association of Asphalt Paving Technologists*, Vol.61, 1992.

**LIST OF TABLES**

Table 1 Material properties of the various layers used in the analysis

Table 2 Deformation of an element in the YZ-transverse plane in the asphalt layer along tire edge

Table 3 Properties of the Burgers Model used in the analysis

Table 4 Results of the Burgers Model under cyclic reversal of stress

**LIST OF FIGURES**

Figure 1 Three-dimensional finite element mesh used in the pavement response analysis. The YZ-plane is the transverse plane and the XZ-plane is the longitudinal plane.

Figure 2 Plan view of the contact area of the three-dimensional mesh used in the pavement analysis.

Figure 3 Critical locations for instability rutting propagation in the transverse YZ-plane under a tire load approaching in the X-direction.

Figure 4 Transverse YZ-plane shear stress at the edge of the wheel path at different longitudinal locations

Figure 5 Longitudinal XZ-plane shear stress along the edge of the tire at different longitudinal locations.

Figure 6 Longitudinal shear deformations depicted qualitatively for an element in the asphalt layer.

Figure 7 Depiction of the visco-elastic Burgers Model.

Figure 8 Loading pattern applied in MathCAD implemented Burgers Model for one-way directional loading.

Figure 9 Loading pattern applied in MathCAD implemented Burgers Model for two-way directional loading.

**TABLE 1 Material Properties of the Various Layers Used in the Analysis**

LAYER	Modulus (MPa)	Poisson's Ratio	Thickness (mm)
Asphalt Concrete	2,071	0.45	100
Base	193		260
LR Stabilized Sub-Base	128	0.45	305
Subgrade	55	0.45	1160

**TABLE 2 Deformation of an Element in the YZ-transverse plane in the Asphalt Layer Along Tire Edge**

Shape of Element in AC Layer, Left Side of Tire Edge	Point of Interest	Shape of Element in AC Layer, Right Side of Tire Edge
	Far Away, Approaching (A)	
	Next to, (B)	
	Far Away, Passed (C)	

**TABLE 3 Properties of the Burgers Model Used in the Analysis**

Property	Value
$R_1$	2.5 Gpa
$\eta_1$	86.33 GPa•sec
$R_2$	0.5 GPa
$\eta_2$	50 GPa•sec

**TABLE 4 Results of the Burgers Model Under Cyclic Reversal of Stress**

Loading Method	Strain (mm/mm)
Two-way (Shear Cycle Reversal)	$5.434 \times 10^{-8}$
One-way (No Shear Cycle Reversal)	$3.219 \times 10^{-6}$

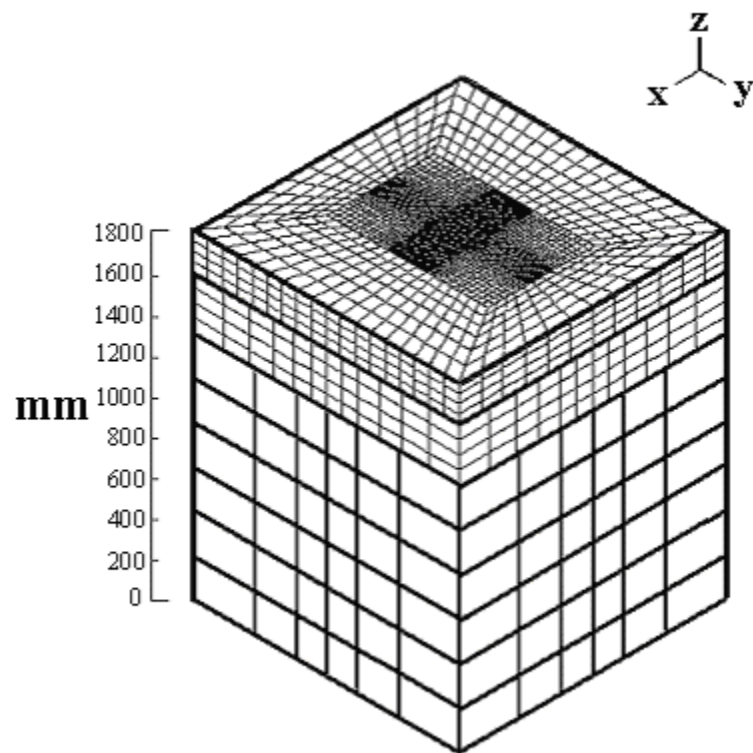


**FIGURE 1** Three-dimensional finite element mesh used in the pavement response analysis. The tire travel is in the positive X direction. The YZ-plane is the transverse plane and the XZ-plane is the longitudinal plane.

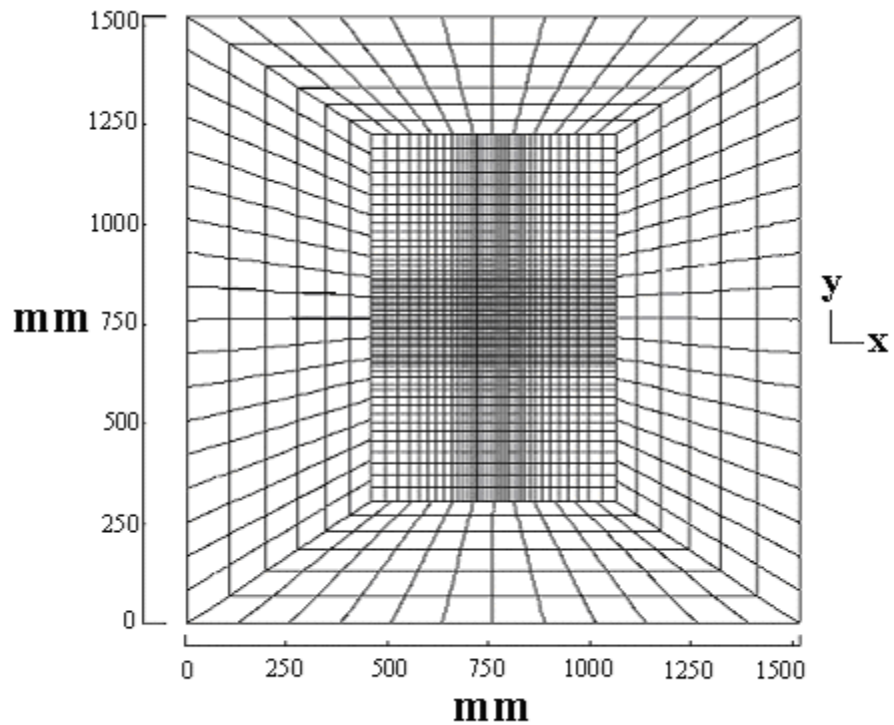


**FIGURE 2** Plan view of the contact area of the three-dimensional mesh used in the pavement analysis. The direction of tire travel is in the positive X direction.

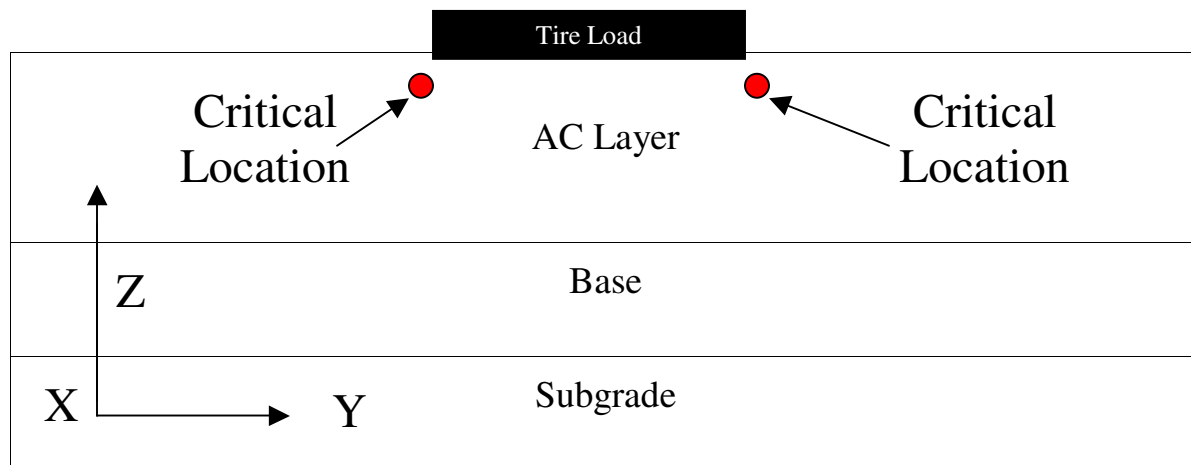


**FIGURE 3** Critical locations for instability rutting propagation in the transverse YZ-plane under a tire load approaching in the X-direction.

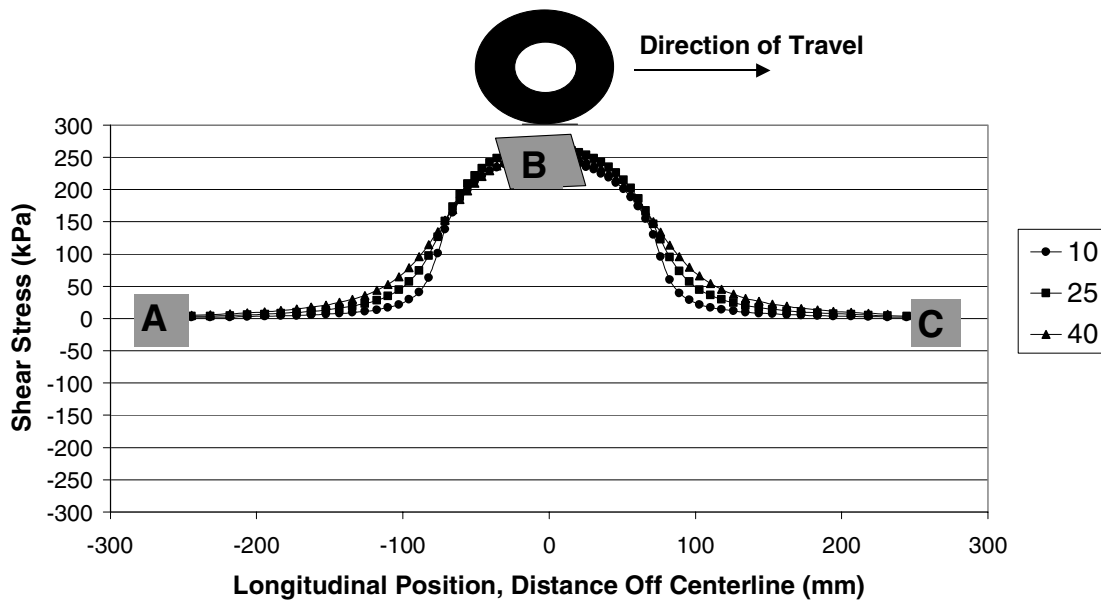


FIGURE 4 Transverse YZ-plane shear stress at the edge of the wheel path at different longitudinal locations.

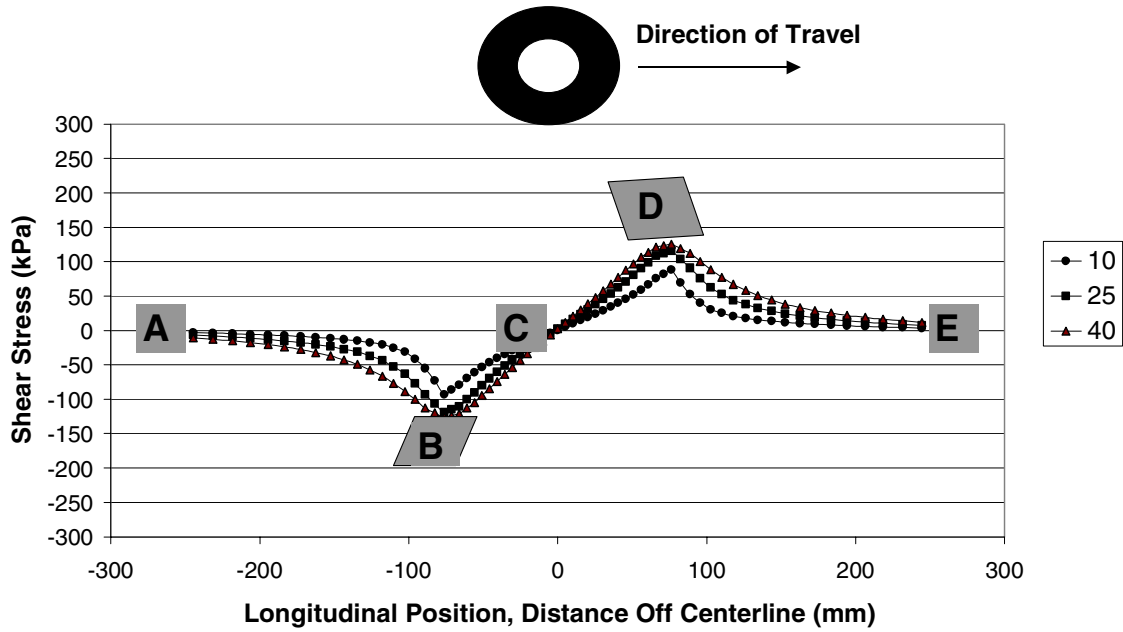
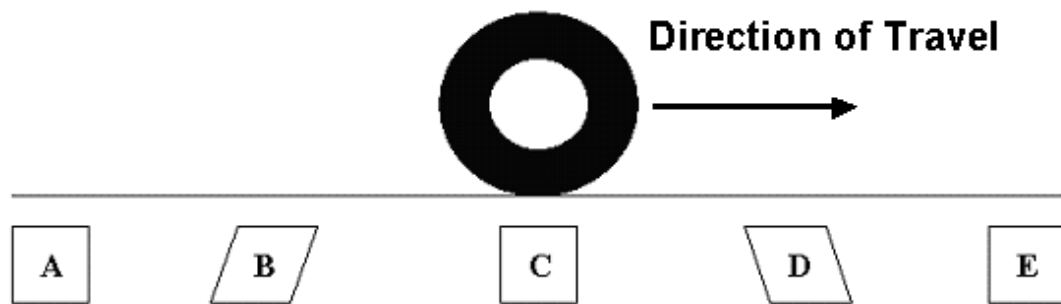


FIGURE 5 Longitudinal XZ-plane shear stress along the edge of the tire at different longitudinal locations.



**FIGURE 6** Longitudinal shear deformations depicted qualitatively for an element in the asphalt layer.

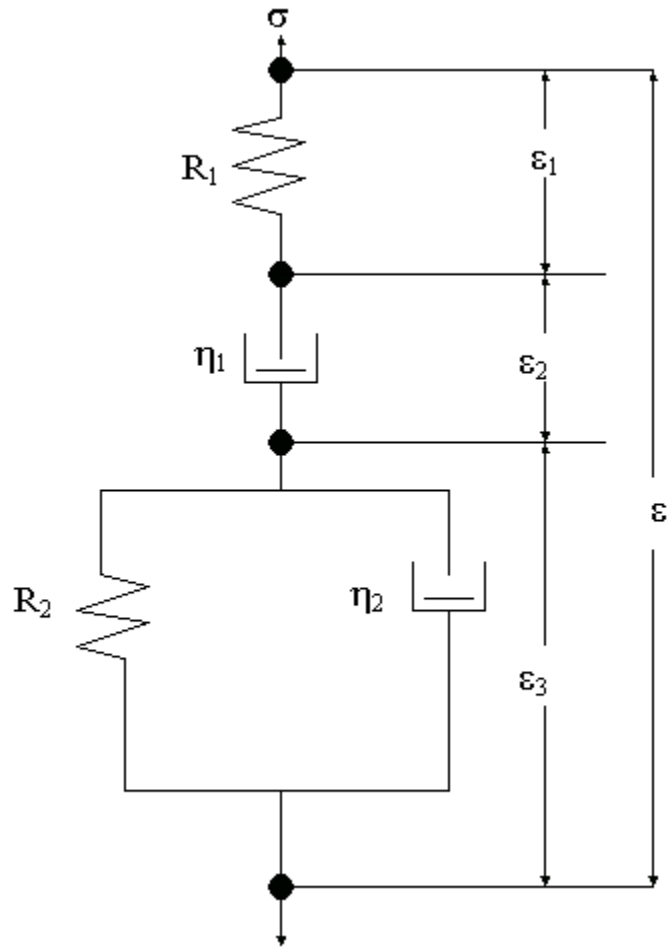
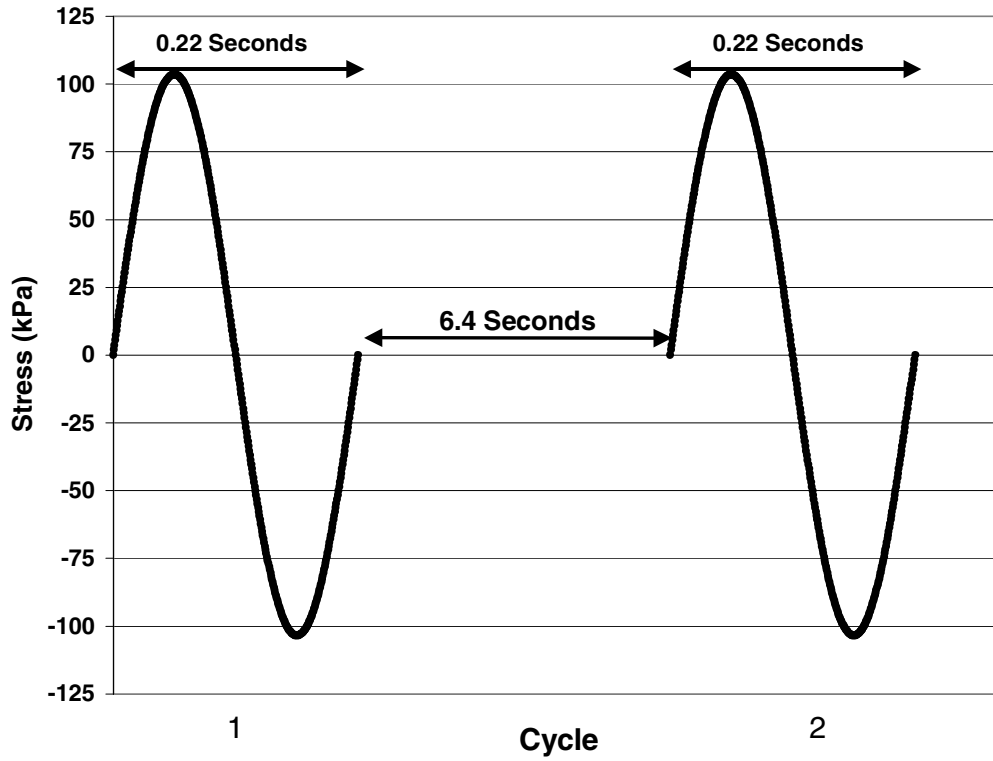
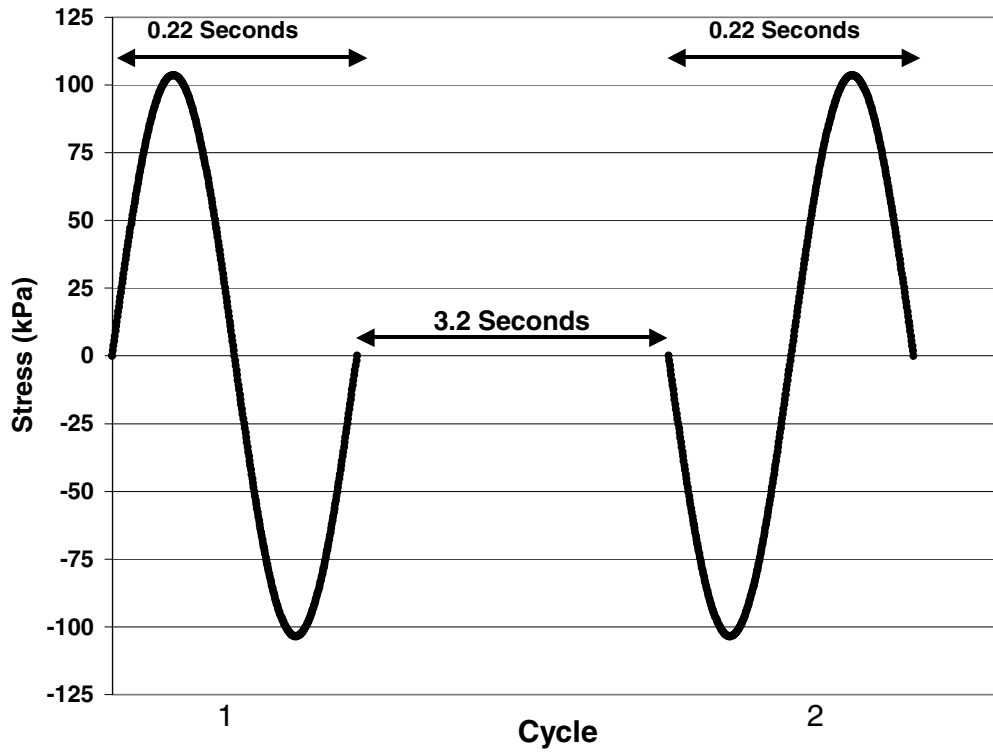


Figure 7 Depiction of the visco-elastic Burgers Model.



**FIGURE 8** Loading pattern applied in MathCAD implemented Burgers Model for one-way directional loading.



**FIGURE 9** Loading pattern applied in MathCAD implemented Burgers Model for two-way directional loading.